Published in Physical Review Letters 94, issue 037403, 1-4, 2005
which should be used for any reference to this work

Optical Phonon Sidebands of Electronic Intersubband Absorption in Strongly Polar Semiconductor Heterostructures

Z. Wang,[1] K. Reimann,[1] M. Woerner,[1,*] T. Elsaesser,[1] D. Hofstetter,[2] J. Hwang,[3] W. J. Schaff,[3] and L. F. Eastman[3]
[1]*Max-Born-Institut für Nichtlineare Optik und Kurzzeitspektroskopie, 12489 Berlin, Germany*
[2]*University of Neuchâtel, Institute of Physics, 2000 Neuchâtel, Switzerland*
[3]*Cornell University, 415 Phillips Hall, Ithaca, New York 14853, USA*

We present the first evidence for a distinct optical phonon progression in the linear and nonlinear intersubband absorption spectra of electrons in a GaN/$Al_{0.8}Ga_{0.2}N$ heterostructure. Femtosecond two-color pump-probe experiments in the midinfrared reveal spectral holes on different vibronic transitions separated by the LO-phonon frequency. These features wash out with a decay time of 80 fs due to spectral diffusion. The remaining nonlinear transmission changes decay with a time constant of 380 fs. All results observed are described by the independent boson model.

The optical line shapes of electronic transitions in condensed matter reflect the ultrafast dynamics of the elementary excitations to which the electrons are coupled. Of particular interest for a broad range of phenomena is the coupling between electrons and nuclear motions, i.e., local vibrational modes and/or phonons.

(i) Coupling to underdamped nuclear motions gives rise to spectrally distinct sidebands in electronic spectra [1]. In molecules, such an interaction with intramolecular modes underlies the vibronic structure of electronic absorption and emission bands, which are additionally broadened by dephasing and spectral diffusion processes originating from a coupling to (overdamped) motions of the fluctuating surroundings [2,3]. In crystalline solids with much more delocalized electronic wave functions and phonon modes, phonon sidebands of electronic transitions have been observed mainly for interband spectra of impurities [1], for quantum-dot-like structures [4–8], and through coherent phonon oscillations modulating the optical reflectivity [9,10].

(ii) Electron-phonon coupling strongly influences the nonequilibrium dynamics of electrons, both in the quantum-kinetic [11] and in the incoherent scattering regimes [12]. Such phenomena occur on femtosecond to picosecond time scales and have been investigated extensively by ultrafast nonlinear spectroscopy.

So far, the majority of investigations of electron-phonon coupling focused on *interband* transitions in solids. The influence of electron-phonon coupling on *intraband* transitions was mainly studied in the context of polaron physics [13,14]. Intraband transitions provide direct access to the nonequilibrium dynamics of electrons. Theoretical studies suggest a prominent role of electron-phonon coupling for the line shape of intraband (free-carrier) absorption and emission. So far, clear experimental signatures of electron-phonon coupling are missing for the line shape of intersubband (IS) transitions (dipole-allowed transitions between quantized conduction subbands [15]), although first theoretical studies predict such polaronic signatures [16].

Because of their strong electron-phonon coupling, nanostructures made from strongly polar materials like group-III nitrides are promising systems for the occurrence of IS phonon sidebands. Because they have large conduction band discontinuities and thus allow IS transitions at short wavelengths, GaN/AlGaN multiple quantum wells have received much interest. Intersubband absorption in such quantum wells has been observed in the spectral range up to the telecommunication wavelength of $\approx 1.55\ \mu$m [17–19]. Recently, IS absorption was also observed in GaN/AlGaN-based high-electron-mobility transistors [20].

In this Letter we show for the first time that linear and particularly nonlinear IS absorption spectra of electrons in a GaN/AlGaN heterostructure show a distinct vibrational progression due to strong polar coupling to optical phonons. In femtosecond two-color pump-probe experiments in the midinfrared we observe during the temporal overlap of pump and probe pulses sharp spectral holes on different vibronic transitions spectrally separated by the LO-phonon frequency. These spectral features wash out after excitation with a decay time of 80 fs due to spectral diffusion. The nonlinear transmission spectrum decays by IS scattering with a time constant of 380 fs.

We investigate a prism-shaped sample [Fig. 1(a)], which was grown on a *c*-face sapphire substrate using molecular beam epitaxy. The layer sequence is 20 nm AlN, 1.2 μm GaN, 13 nm $Al_{0.8}Ga_{0.2}N$, and finally 2 nm GaN as a contact layer. All layers are nominally undoped. For reflection, a gold layer was sputtered onto the contact layer. In this sample, a large piezoelectric field is present at the heterointerface due to the lattice mismatch and the hexagonal crystal structure. The piezoelectric field together with the heterointerface result in a deep triangular well shown in

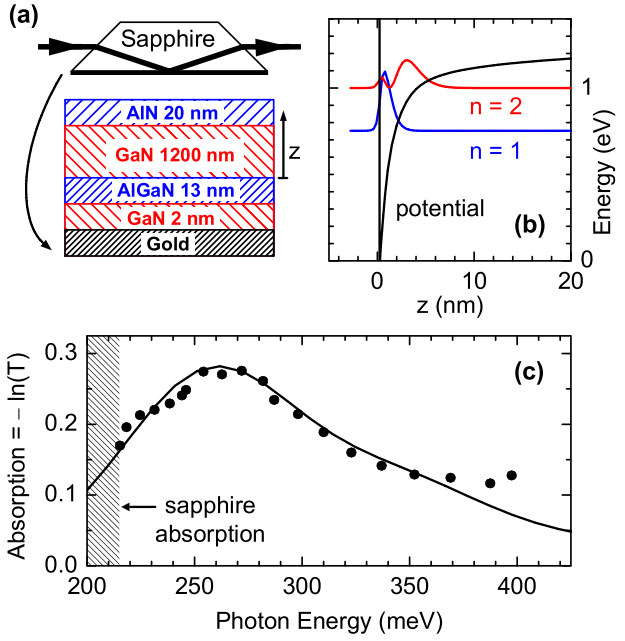

FIG. 1 (color online). (a) Cross section through the prism-shaped sample. (b) Self-consistent calculation of the triangular potential well and the probability densities of the two lowest electron subbands $n = 1$ and $n = 2$ near the GaN/$Al_{0.8}Ga_{0.2}N$ interface. (c) Measured (symbols) and calculated (solid line) absorption spectrum. The broad absorption band is due to transitions of electrons from the $n = 1$ to the $n = 2$ subband in the triangular potential well shown in (b).

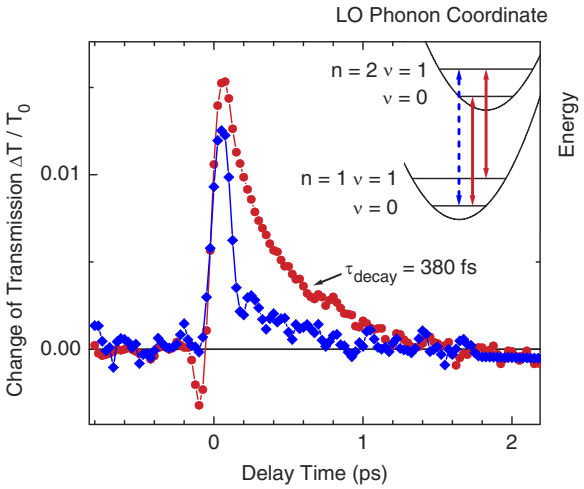

FIG. 2 (color online). Time transients from two-color midinfrared pump-probe experiments for detection energies of $E_{det} = 258$ meV (circles: resonant to $\Delta\nu = 0$ transitions) and $E_{det} = 337$ meV (diamonds: $\Delta\nu = +1$). The transmission change of the GaN/AlGaN sample is plotted as a function of the delay between pump and probe. The pump pulse at 355 meV is resonant to the vibronic transition between $|n = 1, \nu = 0\rangle$ and $|n = 2, \nu = 1\rangle$ in the harmonic potential surfaces of the coupled electron–LO-phonon system shown in the upper right corner.

Fig. 1(b) together with the calculated probability densities of the two lowest electron subbands $n = 1$ and $n = 2$ [20]. The stationary IS absorption spectrum (symbols) measured at a temperature of 300 K is plotted in Fig. 1(c). The broad absorption band is due to transitions of electrons from the $n = 1$ to the $n = 2$ subband. The solid line is the result of the theory, which is described later.

In our time-resolved experiments, electrons are excited from the $n = 1$ to the $n = 2$ subband by bandwidth-limited 100 fs pump pulses, having different center frequencies within the IS absorption band. The nonlinear response in a broad spectral range is measured by independently tunable weak 50 fs probe pulses. Pump and probe pulses at a 1 kHz repetition rate are derived from the output of two synchronized optical parametric amplifiers by difference frequency mixing in 1 mm and 0.5 mm thick GaSe crystals, respectively [21]. After interaction with the sample, the probe pulses are spectrally dispersed in a monochromator (3 meV resolution) and detected by a cooled InSb detector. The coupling to the IS dipole moment is maximized using p-polarized pulses and the prism geometry shown in Fig. 1(a).

We performed an extensive series of time-resolved experiments with pump and probe pulses at different frequencies within the IS absorption band. The most interesting spectral combinations are shown in Figs. 2 and 3. In these measurements the pump pulse is spectrally located at $E_{pump} = 355$ meV [dashed line in Fig. 3(a)], i.e., in the high energy wing of the structureless absorption band. In Fig. 2 we present transients for two prominent detection frequencies, $E_{det} = 258$ meV (circles) and $E_{det} = 337$ meV (diamonds). The transmission change $\Delta T/T_0 = (T - T_0)/T_0$ is plotted as a function of the delay t_D between pump and probe (T, T_0: transmission with and without excitation, respectively).

At the maximum of the linear absorption band the signal (circles) rises within the time resolution and decays subsequently with a time constant of $\tau_{decay} = 380$ fs. For a detection frequency ≈ 20 meV below the pump pulse the signal (diamonds) of similar amplitude shows first a fast decay with a decay time of 80 fs followed by a slow decay with the same time constant $\tau_{decay} = 380$ fs as at the maximum. The amplitude ratio of the two slowly decaying components is similar to that of the linear absorption [Fig. 1(c)] at E_{det}.

Transient IS spectra are shown in Fig. 3. Around $t_D = 0$ we observe two pronounced peaks of nonlinear transmission (spectral holes) separated by the energy of the GaN longitudinal optical phonon $\hbar\omega_{LO} = 92$ meV: one is redshifted relative to the pump pulse by 20 meV, and the second coincides spectrally with the maximum of the linear absorption band. At $t_D = 100$ fs, these spectral features are nearly washed out. For $t_D \geq 200$ fs, the transient spectrum has a constant shape with an amplitude decaying with $\tau_{decay} = 380$ fs [22].

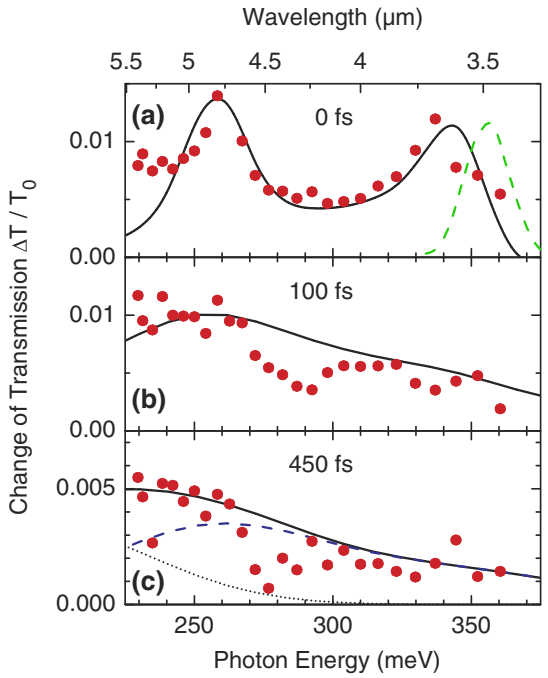

FIG. 3 (color online). Measured (symbols) [22] and calculated (solid line) transient spectra from two-color pump-probe experiments for different delays between pump and probe. (a) The spectrum of the 100 fs pump pulse (dashed line) is shown for comparison. (c) After spectral diffusion the nonlinear transmission spectrum has the shape of the sum of the linear absorption spectrum (dashed line) and the Stokes-shifted gain spectrum (dotted line).

Three experimental findings are important to note: (i) For all measured spectral combinations of E_{pump} and E_{det} we observe a rise of IS bleaching within the time resolution of our experiment ($\approx$50 fs) and a bleaching amplitude depending strongly on E_{det} [cf. Fig. 3(a)]. (ii) For pump energies higher than $E_{\text{pump}} = 275$ meV, a redshifted line shape of the nonlinear transmission occurs relative to the center frequency of the pump pulse for $t_{\text{D}} = 0$. (iii) For fixed E_{pump} and E_{det} data measured with different pump intensities show transients having an *identical shape* with an amplitude depending almost linearly on the excitation density.

Now, we discuss the role of electron-phonon coupling in the linear and nonlinear IS absorption of the strongly polar GaN/$Al_{0.8}Ga_{0.2}N$ heterostructure. A rough estimate of the intrasubband electron-LO-phonon scattering rate according to Fermi's golden rule gives the very high value of $\pi\alpha\omega_{\text{LO}} = 2 \times 10^{14}$ s^{-1} [23] with the dimensionless Fröhlich coupling constant $\alpha = 0.5$ [12], even higher than the phonon angular frequency $\omega_{\text{LO}} = 1.40 \times 10^{14}$ s^{-1}. Because of this strong coupling neither pure electrons nor pure phonons are appropriate quasiparticles. Instead, combined quasiparticles (intersubband polarons), which lead to a sequence of vibronic states (see inset of Fig. 2), are a better description for the underlying physics. These vibronic states, consisting of strongly coupled electrons and LO phonons, couple less strongly to other elementary excitations. The coupling to these other elementary excitations is the cause of the dephasing of the vibronic transitions.

An analytically solvable model for such phenomena is the independent boson model (IBM), mainly applied to molecular systems [7,24–26]. The IBM accounts for both linear and nonlinear optical properties of systems with strong electron-phonon coupling from a phenomenological point of view. It describes the relevant elementary excitations as a thermal bath of harmonic oscillators coupling linearly but with arbitrary strength to the electronic system under consideration. The IBM allows for a quantitative analysis of frequency-resolved nonlinear transmission experiments [27,28], in particular, during the temporal overlap of femtosecond pump and probe pulses.

Using the formalism of [28], we analyze our experiments considering an electronic two-level system strongly coupled to both a prominent phonon mode causing the experimentally observed sidebands and to a continuum of oscillators, representing all other scattering mechanisms, e.g., carrier-carrier scattering and disorder scattering. This continuum of oscillators is equivalent to one strongly overdamped oscillator, the so-called Brownian oscillator [25]. The corresponding combined line shape function $g(t)$ is given by

$$g(t) = -\frac{D^2}{2}[(N+1)(e^{-i\omega_{\text{LO}}t} - 1) + N(e^{i\omega_{\text{LO}}t} - 1)] + \frac{2\lambda k_B T_L}{\hbar\Lambda^2}(\Lambda t - 1 + e^{-\Lambda t}) + i\frac{\lambda}{\Lambda}(1 - e^{-\Lambda t}). \quad (1)$$

The first term is due to the strong polar coupling of the IS transition to the LO phonon in GaN ($\hbar\omega_{\text{LO}} = 92$ meV) with a coupling strength characterized by the dimensionless oscillator displacement D, which is proportional to $\sqrt{\alpha}$. $N = 0.03$ is the thermal population of LO phonons at $T_L = 300$ K. The second and third term stem from the coupling of the IS transition to the Brownian oscillator [25]. This coupling allows one to describe simultaneously the experimentally observed phenomena of electronic dephasing, spectral diffusion, and the time-dependent Stokes shift [3]. It is characterized by the reorganization parameter λ, which is a measure for the integrated displacement of the continuum of oscillators, and by the correlation time Λ^{-1}, which describes the time scale on which spectral diffusion occurs. $g(t)$ allows the calculation of both linear and nonlinear response functions [3,29]. To give two examples, the absorption spectrum $A(\omega)$ is proportional to $\text{Re}\{\omega \int_0^\infty \exp[i(\omega - \omega_{12})t - g(t)]dt\}$, and the gain spectrum is proportional to $\text{Re}\{\omega \int_0^\infty \exp[i(\omega - \omega_{12})t - g^*(t)]dt\}$. ω_{12} is the transition frequency of the uncoupled electronic IS transition.

This model accounts for both the linear absorption spectrum and the full set of nonlinear pump-probe data with the

following parameters: $D = 0.85$, $\hbar\lambda = 35$ meV, $\Lambda^{-1} = 80$ fs, $\hbar\omega_{12} = 225$ meV, and the lifetime of carriers in the $n = 2$ subband $T_1 = 380$ fs (measured value). The calculated spectra are in good agreement with all our experimental results [see, e.g., the solid lines in Figs. 1(c) and 3]. In particular, the position, width, and amplitude of the spectral holes around $t_D = 0$ are well reproduced by the model. The physical mechanism underlying these spectral features is explained in the configurational coordinate drawing [24] of the coupled electron–LO-phonon system [inset of Fig. 2]. The pump pulse is resonant to the vibronic transition between $|n = 1, \nu = 0\rangle$ and $|n = 2, \nu = 1\rangle$ (ν is the vibrational quantum number). This leads to a bleaching on the same transition at $E_{\text{det}} = 337$ meV, slightly redshifted due to the initial motion of the wave packet on the $n = 2$ potential surface [27]. Additionally, one observes a spectral hole around the $\Delta\nu = 0$ transitions due to both gain from the $|n = 2, \nu = 1\rangle$ state and depletion of the $|n = 1, \nu = 0\rangle \leftrightarrow |n = 2, \nu = 0\rangle$ transition.

From the instantaneous transmission increase for all spectral positions E_{det} we conclude that homogenous broadening is an important contribution to the total IS linewidth. In the IBM this corresponds to a very short correlation time Λ^{-1}, which quickly washes out the spectral features around $t_D = 0$ by ultrafast spectral diffusion directly observed in the fast decay of the transient at $E_{\text{det}} = 337$ meV (diamonds in Fig. 2) [30]. It results in a nonlinear spectrum having the shape of the sum of the linear absorption (dashed line) and the emission spectrum (dotted line) [Fig. 3(c)]. In the IBM spectral diffusion causes concomitantly a time-dependent Stokes shift for the photoinduced gain [dotted line in Fig. 3(c)], which dominates the nonlinear response at long wavelengths.

The value of the oscillator displacement D depends on the electron-phonon coupling constant α and on the spatial extent of the electron in-plane wave function. The high value of $D = 0.85$ derived from our data points to a substantial in-plane localization. There are two possible reasons for such a strong localization: On the one hand, the interface has monolayer fluctuations. This static disorder together with the high built-in electric fields of about 8 MV/cm can already cause lateral localization [31,32]. On the other hand, scattering processes can lead to dynamic localization.

In conclusion, the ultrafast IS dynamics of electrons in a GaN/AlGaN heterostructure was studied. Two-color pump-probe measurements display spectral holes spectrally separated by the LO-phonon frequency. These spectral features wash out after excitation with a decay time of 80 fs. The IS scattering time of electrons has a value of 380 fs. Our results are highly relevant for understanding IS dynamics in quantum wells and quantum cascade structures made from highly polar materials.

We thank I. Waldmüller and A. Knorr for valuable discussions. We acknowledge financial support by the Deutsche Forschungsgemeinschaft.

*Electronic address: woerner@mbi-berlin.de

[1] R. E. Dietz, D. G. Thomas, and J. J. Hopfield, Phys. Rev. Lett. **8**, 391 (1962).
[2] C. H. Brito Cruz *et al.*, Chem. Phys. Lett. **132**, 341 (1986).
[3] E. T. J. Nibbering, D. A. Wiersma, and K. Duppen, Chem. Phys. **183**, 167 (1994).
[4] R. W. Schoenlein *et al.*, Phys. Rev. Lett. **70**, 1014 (1993).
[5] D. M. Mittleman *et al.*, Phys. Rev. B **49**, 14 435 (1994).
[6] U. Banin *et al.*, Phys. Rev. B **55**, 7059 (1997).
[7] S. Schmitt-Rink, D. A. B. Miller, and D. S. Chemla, Phys. Rev. B **35**, 8113 (1987).
[8] B. Krummheuer, V. M. Axt, and T. Kuhn, Phys. Rev. B **65**, 195313 (2002).
[9] G. C. Cho, W. Kütt, and H. Kurz, Phys. Rev. Lett. **65**, 764 (1990).
[10] K. J. Yee *et al.*, Phys. Rev. Lett. **88**, 105501 (2002).
[11] L. Bányai *et al.*, Phys. Rev. Lett. **75**, 2188 (1995).
[12] B. K. Ridley, *Quantum Processes in Semiconductors* (Oxford University Press, Oxford, 1993), 3rd ed.
[13] G. Lindemann *et al.*, Phys. Rev. B **28**, 4693 (1983).
[14] Y. J. Wang *et al.*, Phys. Rev. B **64**, 161303(R) (2001).
[15] T. Elsaesser and M. Woerner, Phys. Rep. **321**, 253 (1999).
[16] S. Butscher *et al.*, Phys. Status Solidi B **241**, R49 (2004).
[17] C. Gmachl *et al.*, Appl. Phys. Lett. **77**, 3722 (2000).
[18] D. Hofstetter *et al.*, Appl. Phys. Lett. **83**, 572 (2003).
[19] J. Hamazaki *et al.*, Appl. Phys. Lett. **84**, 1102 (2004).
[20] D. Hofstetter *et al.*, Appl. Phys. Lett. **80**, 2991 (2002).
[21] R. A. Kaindl *et al.*, J. Opt. Soc. Am. B **17**, 2086 (2000).
[22] The spectral dip around 290 meV [Figs. 3(b) and 3(c)] is due to the residual absorption of gaseous CO_2 present in the experimental setup.
[23] S. Das Sarma, in *Hot Carriers in Semiconductor Nanostructures: Physics and Applications*, edited by J. Shah (Academic Press, Boston, 1992), pp. 53–85.
[24] F. E. Williams and M. H. Hebb, Phys. Rev. **84**, 1181 (1951).
[25] S. Mukamel, *Principles of Nonlinear Optical Spectroscopy* (Oxford University Press, New York, 1995).
[26] G. D. Mahan, *Many-Particle Physics* (Kluwer, New York, 2000), 3rd ed.
[27] W. T. Pollard, S.-Y. Lee, and R. A. Mathies, J. Chem. Phys. **92**, 4012 (1990).
[28] W. T. Pollard *et al.*, J. Phys. Chem. **96**, 6147 (1992).
[29] Y. J. Yan and S. Mukamel, J. Chem. Phys. **89**, 5160 (1988).
[30] This fast decay is not caused by the strong coupling between electrons and LO phonons, but it shows the relaxation of the combined quasiparticles caused by their coupling to all other elementary excitations.
[31] A. Thamm *et al.*, Phys. Status Solidi A **180**, 73 (2000).
[32] K. A. Mkhoyana *et al.*, J. Appl. Phys. **95**, 1843 (2004).